Table I. Structure vs. Energy, Charge Density, and Odd-Electron Density Relationships for the Allene Cation Radical, $[C_3H_4]^+$, Calculated by SCF Methods with STO-3G and 4-31G Basis Sets

structure (symmetry)	energy relative to linear-45°-twist, kcal/mol		charge density[c,d]		odd-electron density[d]	
	STO-3G	4-31G	terminal C	central C	terminal C	central C
linear-0°-twist[a] (C_{2v})	5.7	6.2	-0.33 -0.10	+0.12	0.07	0.25
linear-30°-twist (D_2)	1.2	0.9	-0.23	+0.13	0.34	0.27
linear-44.7°-twist[b] (D_2)	0.0	0.0	-0.25	+0.17	0.38	0.20
linear-60°-twist (D_2)	0.7	1.1	-0.30	+0.22	0.43	0.11
linear-90°-twist (D_{2h})	2.0	4.3	-0.32	+0.28	0.50	0.00
bent-90°-twist[a] (C_{2v})	16.7					

[a] All bond lengths are fully optimized. [b] The minimum-energy geometry represents a complete bond lengths and angles optimization. [c] For comparison, the calculated (STO-3G) values for the neutral allene, terminal and central carbon positive charge densities are -0.17 and +0.03, respectively. [d] Taken from SCF calculations using the 4-31G basis sets at STO-3G optimized geometries.

Scheme III

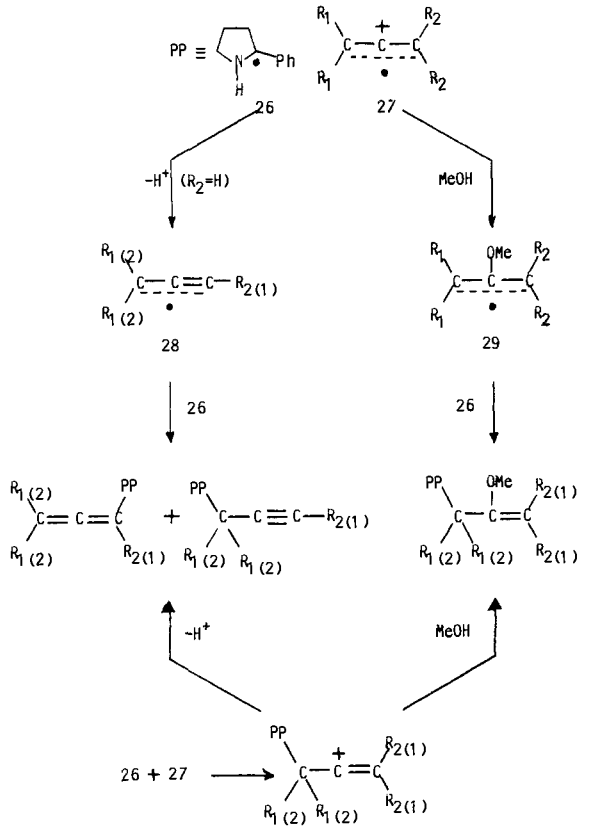

undergo partial or exclusive addition at the more highly substituted terminal positions (e.g., **16** and **17** formation).[13] On the other hand, this position would be favored for addition of **26** to the cation radical **27** ($R_1 = CH_3$; $R_2 = H$) where odd-electron and positive-charge density should be greatest in the alkyl-substituted π-bond.[14,15]

Two final points are worthy of comment. Introduction of strain by incorporating the allene cation radical moiety into a medium-size ring (e.g., **13**) appears to have no effect upon the electronic properties of these systems. Thus, the bending force applied by the $(CH_2)_6$ bridge in $\mathbf{13}^{+\cdot}$ is energetically insufficient to cause adoption of a bent structure with high positive-charge density at the terminal carbons (see Table I). Also, generation of the ketal **18** from photoaddition of **12** to **9** occurs via an initally formed enol ether. The facility of this enol ether to ketal conversion compared to **14**-**16** can be attributed to the lack of α-methyl substitution, which in the latter cases must render the ketal form excessively sterically conjested.

The results summarized above demonstrate the unique potential of electron-transfer-initiated photochemical processes in probing the solution-phase chemistry of interesting charged radical systems. Continuing efforts in this area should clarify the mechanistic questions arising from the current results.

Acknowledgment. Finanical support for this research was provided by grants from the NSF (CHE-09813 and CHE-21125). Helpful discussions with Nathan Bauld are also acknowledged.

(13) (a) Trapping of unsymmetrically substituted allyl radicals should favor the less highly substituted carbons[13b] and of propargyl radicals should lead to both allene and acetylene products.[13c] (b) Ohga, K.; Mariano, P. S. *J. Am. Chem. Soc.* **1982**, *104*, 617 and references therein. (c) Fantazier, R. M.; Pontsma, M. L. *Ibid.* **1968**, *90*, 5490. Poutsma, M. L. *Tetrahedron Lett.* **1969**, 2925. Walling, C.; Heaton, L.; Tanner, D. D. *J. Am. Chem. Soc.* **1965**, *87*, 1715.

(14) The reduced degree of twisting for alkyl-substituted allenes postulated on the basis of the PES results[9b] is confirmed by our SCF (4-31G) calculations, which show a minimized geometry for the 1,1-dimethylallene cation radical having 1° twist angle, respective C_1-C_2 and C_2-C_3 bond lengths of 1.41 and 1.32 Å, and respective C_1, C_2, and C_3 odd-electron densities of 0.28, 0.36, and 0.05 and positive-charge densities of +0.2, +0.16, and -0.09.

(15) (a) An isolated, yet pertinent, observation of a similar nulceophilic addition to the central carbon of a highly phenyl-substituted allene cation radical is presented in a recent report by Johnson.[15b] (b) Klett, B.; Johnson, R. P. *Tetrahedron Lett.* **1983**, 1107.

Nickel and Iron EXAFS of F_{420}-Reducing Hydrogenase from *Methanobacterium thermoautotrophicum*†

Paul A. Lindahl,* Nakao Kojima,*,‡ Robert P. Hausinger,* Judith A. Fox,* Boon K. Teo,*,§ Christopher T. Walsh,* and William H. Orme-Johnson*

Department of Chemistry
Massachusetts Institute of Technology
Cambridge, Massachusetts 02139
AT&T Bell Laboratories, Murray Hill, New Jersey 07974

Received December 19, 1983

Methanobacterium thermoautotrophicum produces two hydrogenases containing nickel and iron,[1,2] which are thought to catalyze the H_2-linked assimilation of CO_2 required for energy-yielding methanogenesis[3,4] in this organism. We recently detected a nitrogen atom ≥3.5 Å from the nickel site in the F_{420} deazaflavin reducing hydrogenase[1] using electron spin echo spectroscopy.[5]

† Supported in part by NIH Grant GM 31574 and NSF Grant 8205764-PCM.

‡ Present address: Institute of Applied biochemistry, Yagi Memorial Park, Gifu, Japan 505-01.

§ AT&T Bell Laboratories, Murray Hill, New Jersey 07974.

(1) Jacobson, F. S.; Daniels, L.; Fox, J. A.; Walsh, C. T.; Orme-Johnson, W. H. *J. Biol. Chem.* **1982**, *257*, 3385-3388.

(2) Kojima, N.; Fox, J. A.; Hausinger, R. P.; Daniels, L.; Orme-Johnson, W. H.; Walsh, C. *Proc. Natl. Acad. Sci. U.S.A.* **1983**, *80*, 378-382.

(3) Daniels, L.; Fulton, G.; Spencer, R. W.; Orme-Johnson, W. H. *J. Bacteriol.* **1980**, *141*, 694-698.

(4) Spencer, R. W.; Daniels, L.; Fulton, G.; Orme-Johnson, W. H. *Biochemistry* **1980**, *19*, 3678-3683.

0002-7863/84/1506-3062$01.50/0

Table I. Summary of F_{420} Hydrogenase EXAFS Results[a]

compound	bond	bond distance, Å	coord no.	Debye–Waller factor, Å
Ni(toluene-3,4-dithiolato)$_2^{2-}$	Ni–S	2.19 ± 0.04	4	0.060 ± 0.025
F_{420} hydrogenase	Ni–S	2.25 ± 0.04	2.9	0.090 ± 0.022
$(Et_4N)_2Fe_4S_4(SPh)_4$	Fe–S	2.27 ± 0.03	4	0.055 ± 0.028
F_{420} hydrogenase	Fe–S	2.26 ± 0.03	3.6	0.055 ± 0.026
$(Et_4N)_2Fe_4S_4(SPh)_4$	Fe–Fe	2.74 ± 0.03	3	0.060 ± 0.040
F_{420} hydrogenase	Fe–Fe	2.73 ± 0.03	2.1	0.103 ± 0.050

[a] The σ^*, S*, and ΔE_0^* obtained from the unrestricted fit of the $(NEt_4)_2[Fe_4S_4(SPh)_4]$ filtered data were 0.055 Å, 0.495, and 4.73 eV for Fe–S and 0.060 Å, 0.37, and 0.01 eV for Fe–Fe. The listed model compound coordination numbers were assumed. A ΔE_0^* of 7.9 eV for Ni–S was estimated by extrapolation of the ΔE_0^* for Fe–S. σ^* and S* for Ni–S were 0.067 Å and 0.593. Coordination number errors were estimated at ca. 20%.[23]

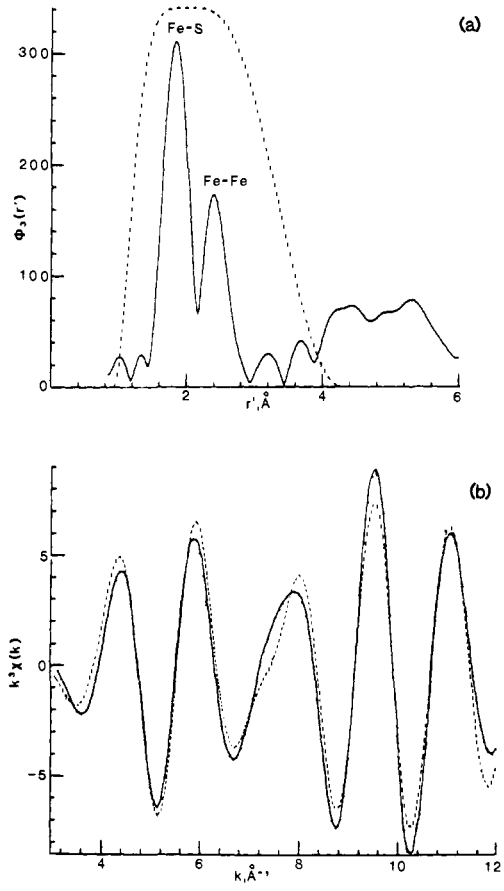

Figure 1. Fourier transform (a) and filtered data (b) of the $k^3\chi(k)$ vs. k EXAFS spectrum from the iron edge of F_{420} hydrogenase. The dashed curve in the Fourier transform is the window function used in Fourier filtering while that in the filtered data is the two-term theoretical fit.

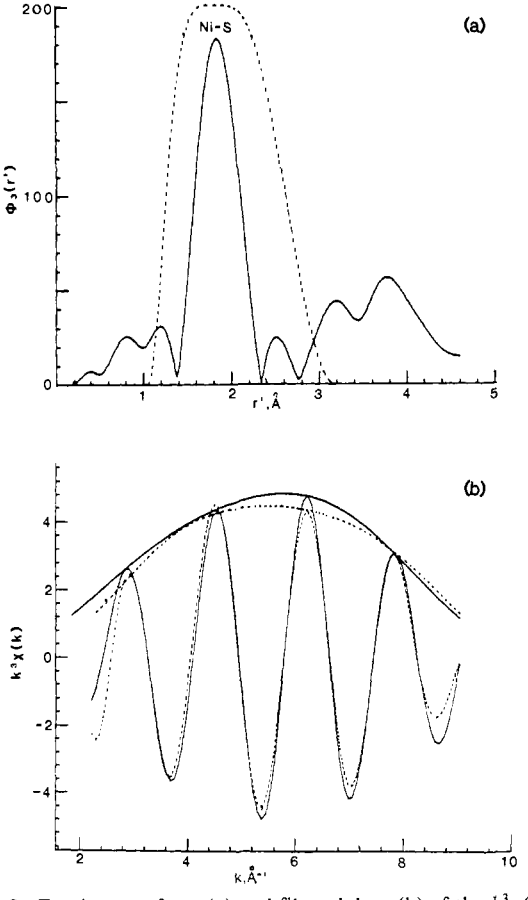

Figure 2. Fourier transform (a) and filtered data (b) of the $k^3\chi(k)$ vs. k EXAFS spectrum from the nickel edge of F_{420} hydrogenase. The amplitude functions for the filtered data and fit are shown.

Here we characterize the average ligand environments of nickel and iron in a stable oxidized state of this enzyme using the EXAFS technique.

Nickel and iron K-edge X-ray absorption measurements were made using the fluorescence technique at the Cornell High Energy Synchrotron Source on the C1 beam line.[6] The samples were kept at ca. 160 K with a cryostat.[7] Cobalt and manganese filters for the nickel and iron edges were used in conjunction with the detector.[8] The purified hydrogenase[1] containing 1.7 mM Ni and ca. 43 mM Fe had a specific activity of 37 (μmol/min)/mg before and 30 (μmol/min)/mg after the experiment.

The analyses were performed according to the method of Teo[9-11] on the average of 10 nickel and two iron EXAFS spectra, truncated at 8.8 and 12 Å^{-1} respectively. After subtraction of a four-segment background spline and multiplication by k^3, the data were Fourier transformed, Fourier filtered (nickel window, 2.2 Å; iron window, 3.0 Å), and fit in k space to the theoretical phase and amplitude functions of Teo and Lee.[11] The model compounds Ni(toluene-3,4-dithiolato)$_2^{2-}$[12] and $(NEt_4)_2[Fe_4S_4(SPh)_4]$[13] were similarly analyzed (Table I) and were used where possible to refine distance and coordination numbers according to the fine adjustment based on models (FABM) method.[14]

(5) Tan, S. L.; Fox, J. A.; Kojima, N.; Walsh, C. T.; Orme-Johnson, W. H. *J. Am. Chem. Soc.*, following paper in this issue.
(6) Batterman, B. W. In "EXAFS Spectroscopy: Techniques and Applications"; Teo, B. K,, Joy, D. C., Eds.; Plenum Press: New York, 1981; pp 197–204.
(7) Johnson Research Foundation, University of Pennsylvania, Philadelphia, PN.
(8) The EXAFS Co., Seattle, WA. Also, see: Stern, E. A.; Heald, S. M. *Rev. Sci. Instrum.* **1979**, *50*, 1579–1582.
(9) Teo, B. K. In "EXAFS Spectroscopy: Techniques and Applications"; Teo, B. K., Joy, D. C., Eds.; Plenum Press: New York, 1981; pp 13–58.
(10) Teo, B. K. *Acc. Chem. Res.* **1980**, *13*, 412–419.
(11) Teo, B. K.; Lee, P. S. *J. Am. Chem. Soc.* **1979**, *101*, 2815–2832.
(12) (a) Gray, H. B.; Billig, E. *J. Am. Chem. Soc.* **1963**, *85*, 2019–2020. (b) Williams, R.; Billig, E.; Waters, J. H.; Gray, H. B. *Ibid.* **1966**, *88*, 43–50. (c) Baker-Hawkes, M. J.; Billig, E.; Gray, H. B. *Ibid.* **1966**, *88*, 4870–4875.
(13) Averill, B. A.; Herskovitz, T.; Holm, R. H.; Ibers, J. A. *J. Am. Chem. Soc.* **1973**, *95*, 3523.
(14) Teo, B. K.; Antonio, M. R.; Averill, B. A. *J. Am. Chem. Soc.* **1983**, *105*, 3751–3762.

The first and second peaks in the Fourier transform of the iron edge EXAFS (Figure 1) fit unequivocally to sulfur and iron (Table I). Unfortunately, the coordination number derived from this and other EXAFS analyses are quite sensitive to the Debye-Waller factor, which we cannot determine very precisely (Table I). The Fe-Fe coordination number may be less accurate than the Fe-S number since apparent differences in the relevant Debye-Waller factors between the enzyme and model are larger in the former case. We conclude that there are iron-sulfur clusters in this hydrogenase with Fe-S and Fe-Fe distances nearly identical with those found in well-characterized iron-sulfur proteins and model compounds.

The Fourier transform of the nickel EXAFS (Figure 2a) contains one major peak, which was isolated by Fourier filtering. The amplitude and phase functions of the peak could be fit to sulfur (Figure 2b) but not to nitrogen (or oxygen). An apparently reasonable fit to nitrogen could be constructed only by distorting the nitrogen phase function by setting ΔE_0 to 30; this behavior was also observed in attempts to fit Ni(toluene-3,4-dithiolato)$_2^{2-}$ to nitrogen. Thus we conclude that sulfur is the *dominant* scatterer in the nickel EXAFS in F_{420}-reducing hydrogenase. The Debye-Waller factors of the model and protein are again apparently somewhat different, diminishing our confidence in the accuracy of the Ni-S coordination number.

The distance of 2.19 Å obtained for Ni(toluene-3,4-dithiolato)$_2^{2-}$ is as would be expected for a square-planar Ni(II) complex[15] and is close to the average distance of 2,168 Å found in the equivalent square-planar cobalt species.[16] An estimate of ca. 1.3 Å for the covalent radius of low-spin Ni(III) was obtained from the crystal structure of $Ni^{III}[C_6H_3(CH_2NMe_2)_2\text{-}1,5]I_2$,[17] while a value of ca. 1.2 Å has been calculated from $Ni^{III}Br_3(PPhMe_2)_2$.[17,18] Using 1.04 Å as a sulfur covalent radius,[19] the distance of 2,25 Å observed in the enzyme is within the expected region.

The positions of the EPR g values in the enzyme suggest the nickel is low-spin Ni(III)[2] with the unpaired electron in an orbital of d_{z^2} symmetry[20-22] and it has been suggested on this basis that the nickel in a hydrogenase in crude membrane fractions from *Methanobacterium bryantii* is a rhombically distorted octahedron.[20] Similarly, square-pyramidal geometry is also possible. The crystal structure and EPR of the low-spin square-pyramidal nickel(III) complex $Ni^{III}[C_6H_3(CH_2NMe_2)_2\text{-}1,5]I_2$[17] provides solid evidence for this possibility.

In summary, the iron EXAFS indicates the presence of iron-sulfur clusters. The dominant scatterers in the nickel EXAFS comprised approximately three sulfur atoms at ca. 2.25 Å. Our inability to fit a nitrogen or oxygen scatterer at a distance of around 2.0 Å to the EXAFS suggests that none are present, though a minor contribution may have gone undetected. In addition, the distant nitrogen observed by electron spin echo spectroscopy[5] was not detected. As a working hypothesis, we suggest the nickel in F_{420}-reducing hydrogenase has equatorial sulfurs with either one or two loosely held axial ligands in roughly a tetragonally distorted octahedron or square pyramid. Further work aimed at identifing other ligand atoms is in progress.

(15) Davis, P. H.; White, L. K.; Belford, R. L. *Inorg. Chem.* **1975**, *14*, 1753-1757. Eisenberg, R. *Prog. Inorg. Chem.* **1970**, *12*, 295.
(16) Eisenberg, R.; Dori, Z.; Gray, H. B.; Ibers, J. A. *Inorg. Chem.* **1968**, *7*, 741-748.
(17) Grove, D. M.; van Koten, G.; Zoet, R.; Murrall, N. W.; Welch, A. J. *J. Am. Chem. Soc.* **1983**, *105*, 1379.
(18) Stalik, J. K.; Ibers, J. A. *Inorg. Chem.* **1970**, *9*, 453-458.
(19) Pauling, L. "The Nature of the Chemical Bond"; Cornell University Press: Ithaca, NY, 1960; Chapter 7.
(20) Lancaster, J. R. *Science (Washington, D.C.)* **1982**, *216*, 1324-1325.
(21) Maki, A. H.; Edelstein, N.; Davison, A.; Holm, R. H. *J. Am. Chem. Soc.* **1964**, *86*, 4580.
(22) Lappin, A. G.; Murray, C. K.; Margerum, D. W. *Inorg. Chem.* **1978**, *17*, 1630-1634.
(23) Eisenberger, P.; Lengeler, B. *Phys. Rev.* **1980**, *22* (8), 3551-3562.

Nickel Coordination in Deazaflavin and Viologen-Reducing Hydrogenases from *Methanobacterium thermoautotrophicum*: Investigation by Electron Spin Echo Spectroscopy

Swee Lian Tan, Judith A. Fox, Nakao Kojima, Christopher T. Walsh, and William H. Orme-Johnson*

Department of Chemistry
Massachusetts Institute of Technology
Cambridge, Massachusetts 02139

Received October 31, 1983

Two hydrogenases that differ in their in vitro activities[1] have recently been purified from *Methanobacterium thermoautotrophicum* (strain ΔH). In vitro, one hydrogenase (FH_2ase) catalyzes the reduction of the physiological two-electron acceptor 7,8-didemethyl-8-hydroxy-5-deazaflavin (F_{420}) by hydrogen, whereas the other has only been observed to reduce the artificial one-electron acceptor methylviologen. Both enzymes, on isolation, contain nickel and iron sulfur clusters and show an essentially superimposable CW EPR spectrum for the nickel paramagnet at 77 K.[1] The FH_2ase has 1 equiv of bound FAD, which seems to be absent from the viologen-reducing enzyme (MVH_2ase). Using electron spin echo spectroscopy, we demonstrate here that the environments of the nickel paramagnet in these two enzymes are in fact different.

The presence of a tightly bound paramagnetic nickel center in both hydrogenases has been confirmed by the hyperfine coupling in the CW EPR powder spectra of the ^{61}Ni enriched enzymes.[2] The powder spectra of the hydrogenases with natural abundance ^{58,60}Ni appear almost identical, but the features are broad enough that small hyperfine splittings are not resolved.[2] However, these splittings can be measured and the identification of nuclei that are more loosely coupled to the electron spin can be made by the technique of electron spin echo envelope modulation (ESEEM).[3]

ESEEM measurements do show a clear difference between the two hydrogenases: the F_{420}-reducing hydrogenase is found to have a nitrogen (^{14}N, I = 1) nucleus near the paramagnetic nickel center whereas this interaction is absent in the methylviologen-reducing hydrogenase.

It has been observed in three-pulse ESEEM experiments (Figure 1)[4] in solids that as the time between the second and third pulses (T) is increased, there is a decrease in the echo intensity due to electron spin relaxation processes. Often superimposed on this decay is a periodic modulation of echo intensity, due to nuclei coupled to the electron spin. The depth and frequencies of components of this modulation convey information as to the identity of nearby nuclei, their number, and the distance separating them from the electron spin. Consequently, a combination of EPR, ENDOR, and ESEEM studies probe directly the immediate magnetic environment of a paramagnet, Mims has shown how the echo modulation amplitude depends on nuclear spin eigenvalues and eigenvectors.[5]

The three-pulse ESEEM patterns for the F_{420}-reducing hydrogenase and the methylviologen-reducing hydrogenase are shown in Figure 1. The difference between the patterns can be explained by the presence of a nitrogen-14 nucleus near the paramagnetic center in FH_2ase. The Fourier transform of the time-domain pattern of FH_2ase has three sharp lines at 0.4, 1.2, and 1.6 MHz

(1) Jacobson, F. S.; Daniels, L.; Fox, J. A.; Walsh, C. T.; Orme-Johnson, W. H. *J. Biol. Chem.* **1982**, *257*, 3385-3398.
(2) Kojima, N.; Fox, J. A.; Hausinger, R. P.; Daniels, L.; Orme-Johnson, W. H.; Walsh, C. T. *Proc. Natl. Acad. Sci. U.S.A.* **1983**, *80*, 378-382.
(3) (a) Mims, W. B.; Peisach, J. *Biol. Magn. Reson.* **1981**, *3*, 213-263. (b) Kevan, L. "Time Domain Electron Spin Resonance"; Kevan, L., Schwartz, R. N., Eds.; John Wiley and Sons: New York, 1979; 279-341. (c) Isoya, J.; Bowman, M. K.; Norris, J. R.; Weil, J. A. *J. Chem. Phy.* 1983, *78*, 1735-1746.
(4) Details of this spectrometer will be published elsewhere: Tan, S. L.; Waugh, J. S.; Orme-Johnson, W. H. *J. Chem. Phys.*, in press.
(5) (a) Mims, W. B. *Phys. Rev. B* **1972**, *5*, 2405; (b) *Ibid.* **1972**, *6*, 3543.

0002-7863/84/1506-3064$01.50/0